



# The *KCNJ11*-E23K Gene Variant Hastens Diabetes Progression by Impairing Glucose-Induced Insulin Secretion

Gregor Sachse,<sup>1</sup> Elizabeth Haythorne,<sup>1</sup> Thomas Hill,<sup>1</sup> Peter Proks,<sup>1,2</sup> Russell Joynson,<sup>3</sup> Raul Terrón-Expósito,<sup>1</sup> Liz Bentley,<sup>3</sup> Stephen J. Tucker,<sup>2</sup> Roger D. Cox,<sup>3</sup> and Frances M. Ashcroft<sup>1</sup>

*Diabetes* 2021;70:1145–1156 | <https://doi.org/10.2337/db20-0691>

**The ATP-sensitive K<sup>+</sup> (K<sub>ATP</sub>) channel controls blood glucose levels by coupling glucose metabolism to insulin secretion in pancreatic β-cells. E23K, a common polymorphism in the pore-forming K<sub>ATP</sub> channel subunit (*KCNJ11*) gene, has been linked to increased risk of type 2 diabetes. Understanding the risk-allele-specific pathogenesis has the potential to improve personalized diabetes treatment, but the underlying mechanism has remained elusive. Using a genetically engineered mouse model, we now show that the K23 variant impairs glucose-induced insulin secretion and increases diabetes risk when combined with a high-fat diet (HFD) and obesity. K<sub>ATP</sub>-channels in β-cells with two K23 risk alleles (KK) showed decreased ATP inhibition, and the threshold for glucose-stimulated insulin secretion from KK islets was increased. Consequently, the insulin response to glucose and glycemic control was impaired in KK mice fed a standard diet. On an HFD, the effects of the KK genotype were exacerbated, accelerating diet-induced diabetes progression and causing β-cell failure. We conclude that the K23 variant increases diabetes risk by impairing insulin secretion at threshold glucose levels, thus accelerating loss of β-cell function in the early stages of diabetes progression.**

Numerous genome-wide association studies have demonstrated that a common polymorphism (E23K) in the *KCNJ11* gene is linked to increased risk of type 2 diabetes (T2D) in Caucasian, Asian, and Arabian populations (1). Initial studies identified the polymorphism but failed to

detect an association with T2D due to the small sample size (2). This is because although the increase in risk is highly significant ( $P = 4 \times 10^{-25}$  by meta-analysis [1]), its effect size is relatively modest (odds ratio [OR] 1.18 for the EK, OR 1.65 for the KK genotype [3]) and can only be detected in large-scale studies or meta-analysis studies (1,3,4). Approximately 58% of Caucasians carry a K risk allele (EK or KK), with 13% being of the KK genotype (3). A similar (>20%) allelic frequency is found in Asian and Arabian populations (4,5). Consequently, the effect on the global population risk is substantial.

The *KCNJ11* gene encodes the main subunit (Kir6.2) of the ATP-sensitive K<sup>+</sup> (K<sub>ATP</sub>) channel in pancreatic β-cells, which plays a key role in glucose homeostasis by coupling glucose metabolism to insulin secretion (6,7). At low plasma glucose levels, K<sub>ATP</sub> channel activity keeps the membrane hyperpolarized, preventing electrical activity and insulin release. Enhanced β-cell glucose metabolism at stimulatory plasma glucose concentrations elevates cytosolic ATP, which binds to the K<sub>ATP</sub> channel, causing it to close. This triggers electrical activity and insulin secretion.

The β-cell K<sub>ATP</sub> channel is composed of four pore-forming Kir6.2 subunits and four regulatory SUR1 subunits (encoded by the *ABCC8* gene), which together form an octameric complex. Activating mutations in *KCNJ11* or *ABCC8* are a common cause of neonatal diabetes (8–13). These mutations impair the ability of MgATP to close the K<sub>ATP</sub> channel, thereby preventing insulin secretion in response to an elevation of blood glucose (8,13,14). There is

<sup>1</sup>Department of Physiology, Anatomy and Genetics, University of Oxford, Oxford, U.K.

<sup>2</sup>Department of Physics, University of Oxford, Oxford, U.K.

<sup>3</sup>Mammalian Genetics Unit and Mary Lyon Centre, MRC Harwell Institute, Oxfordshire, U.K.

Corresponding author: Gregor Sachse, [gregor.sachse@dpag.ox.ac.uk](mailto:gregor.sachse@dpag.ox.ac.uk)

Received 1 July 2020 and accepted 5 February 2021

This article contains supplementary material online at <https://doi.org/10.2337/figshare.13724113>.

© 2021 by the American Diabetes Association. Readers may use this article as long as the work is properly cited, the use is educational and not for profit, and the work is not altered. More information is available at <https://www.diabetesjournals.org/content/license>.

a positive correlation between the molecular and systemic phenotypes, with mutations that cause the largest reduction in ATP sensitivity producing a more severe clinical phenotype (15,16). Mutations that produce a lesser reduction in ATP sensitivity are often associated with transient neonatal diabetes (10), and in some patients, diabetes may not present until later life (17–19).

Although the link between the E23K polymorphism and T2D risk has been known for more than two decades (20), the underlying mechanism has remained largely obscure. Data from several genome-wide association studies suggest that it is the initial transition from healthy glycemic control to impaired glucose tolerance that is mainly affected by the E23K polymorphism (4,21), but with the caveat that there is significant heterogeneity between studies (interstudy heterogeneity  $P < 0.001$ ) (1). On a smaller scale, functional studies have shown that in people with normal glucose tolerance, the K variant is associated with a marked (40%) reduction in insulin secretion in response to an oral or intravenous glucose challenge (22). Other studies have also reported impaired insulin (or C-peptide) secretion in response to oral or intravenous glucose and lower fasting insulin levels (21,23). However, these findings are not universal, as no significant difference in insulin or C-peptide release was found in some studies (24,25).

The role of the Kir6.2-E23 residue in  $K_{ATP}$  channel function has proved equally elusive. The N-terminal first 32 residues of the Kir6.2 subunit are unresolved in all cryo-electron microscopy structures known to date (26–29), and biophysical studies of recombinant Kir6.2-E23K channels heterologously expressed in non- $\beta$ -cells have produced conflicting data. Some studies found the K variant to be associated with a very small reduction in sensitivity to inhibition by ATP, in both the absence (22,30) and presence of  $Mg^{2+}$  (22,31). An increased open probability was reported to underlie the reduced ATP sensitivity (22,30). In contrast, other studies failed to observe a change in open probability (32). Moreover, the decrease in ATP inhibition does not always reach significance (33), and some studies have reported no effect of the K variant on the MgATP sensitivity of the  $K_{ATP}$  channel (34). Similarly, increased activation by MgADP of Kir6.2-K23 channels was observed in one study (31) but not in another (34). Enhanced activation of Kir6.2-K23 channels by long-chain acyl-CoAs has also been observed (32). These data suggest that the Kir6.2-K23 variant has only a small effect on the ATP sensitivity of the  $K_{ATP}$  channel that may not reach significance in some studies.

A further complication is that the E23K polymorphism is in strong linkage disequilibrium both with a second missense polymorphism in *KCNJ11* (I337V) (20) and a missense polymorphism in *ABCC8* (S1369A) (35). More than 72% of individuals with the Kir6.2-E23K allele also carry the Kir6.2-I337V variant, although the link to diabetes risk is stronger for E23K than for I337V (20) or other known Kir6.2 variants (36). Linkage disequilibrium between S1369A and E23K arises because *KCNJ11* and

*ABCC8* lie adjacent on chromosome 11. In one Caucasian population, linkage disequilibrium was almost complete ( $r^2 = 0.98$ ) (36). Lower degrees of linkage disequilibrium have been found in other populations ( $r^2 = 0.56$ ) (1), but the sample size was too small to separate S1369A and E23K effect sizes statistically. A key question, therefore, is whether the observed functional effects are mediated by a single polymorphism or require the combination of two or all three variants. Biophysical studies in heterologous expression systems found functional effects of SUR1-A1369 on  $K_{ATP}$  channel function, implicating a role for SUR1-S1369A in T2D risk (34,37).

In summary, while there is unequivocal evidence that the Kir6.2-K23/SUR1-A1369 haplotype is linked to T2D, it is far from clear whether this is due to the E23K polymorphism in *KCNJ11* or the S1369A variant in *ABCC8* (or both). It is also unclear how the variant enhances diabetes risk and at what stage of diabetes progression and etiology it exerts its main effect. We therefore aimed to address these questions using a genetically engineered mouse model and specifically to determine whether the K23 variant in *KCNJ11* alone is sufficient to cause glucose intolerance and/or diabetes, whether the diabetes results from impaired insulin secretion or action, and whether the variant enhances the risk of diabetes on a high-fat diet (HFD).

## RESEARCH DESIGN AND METHODS

### Animals

The C57BL/6NTac-Kcnj11<sup>em1H</sup>/H (*Kcnj11-K23*) allele was generated using clustered regularly interspaced short palindromic repeats (CRISPR)-aided genome editing technology (38), and heterozygous EK mice were maintained by backcrossing to the same C57BL/6NTac genetic background on which the allele was generated (datasheet available online, DOI: 10.6084/m9.figshare.12200909). Homozygous experimental EE and KK mice were bred as littermates from heterozygous EK  $\times$  EK matings. Phenotyping pipelines and animal maintenance are described in detail in the Supplementary Material Part 1. Litters were randomized, litter size was standardized, and experiments were random order and genotype-blinded. Animal experiments and maintenance were in accordance with UK Home Office guidelines and Animals Scientific Procedures Act (2012) regulations and were approved by the Medical Research Council Harwell Institute Animal Welfare and Ethical Review Board. The diets used were as follows. The standard diet (SD) (RM3; Special Diets Services; Dietex, Witham, U.K.) contained 11.5 kcal% fat (92% of fatty acids  $\geq$  C16), 23.9 kcal% protein, and 61.6 kcal% carbohydrate. The HFD (D12492; Research Diets, New Brunswick, NJ) contained 60.0 kcal% fat (99%  $\geq$  C16), 20.0 kcal% protein, and 20.0 kcal% carbohydrate.

### Blood Glucose Experiments and Glycated Hemoglobin

Free-fed blood glucose was measured (1–4 P.M.) on weeks 7, 9, 11, 13, 15, 17 (SD and HFD) and 28 (HFD). Glycated

hemoglobin (HbA<sub>1c</sub>) was measured after terminal bleeds at 28 weeks using a degradation resistant assay (#80310; Crystal Chem). For intraperitoneal glucose tolerance tests (IPGTT), 2 g glucose/kg body weight (kg<sub>BW</sub>) was injected after an overnight fast. For intraperitoneal insulin tolerance tests (IPITT) at 16 weeks, 0.75 IU/kg<sub>BW</sub> (females) and 1.0 IU/kg<sub>BW</sub> (males) was injected after a 4-h fast.

### Islet Electrophysiology and Glucose-Stimulated Insulin Secretion

Islets were isolated essentially as previously described (39,40). K<sub>ATP</sub> currents were recorded from excised inside-out patches at -60 mV under symmetrical K concentrations, as described (14). Individual MgATP concentration-response curves were fit with the Hill equation, and the mean IC<sub>50</sub> was calculated as the mean of individual fits. For glucose-stimulated insulin secretion (GSIS), islets were used after overnight culture and preincubated for 1 h in low glucose solution (2 mmol/L). Insulin secretion was measured in 1-h batch incubations, and the total insulin content per batch was measured after sonication/acid-ethanol extraction. Insulin was quantified by ELISA (10-1247-10; Merckodia).

### Statistics

GraphPad Prism 8, OriginPro 9.1, and Microsoft Excel 2010 were used for analysis and plotting. Statistical tests used are indicated in the figure legends. *P* values of ≤0.05 were considered statistically significant. A capital *N* is used to denote a single animal, a lower-case *n* to denote the number of membrane patches or batches of islets.

### Data and Resource Availability

The data sets generated and analyzed during the current study are available under DOI:10.6084/m9.figshare.12272873 and DOI:10.6084/m9.figshare.12420839 from figshare.com.

C57BL/6NTac-Kcnj11<em1H>/H mice are available from the European Mouse Mutant Archive (EMMA: www.infrafrontier.eu, repository number EM:12523).

## RESULTS

### E23K Mouse Model Generation

We used CRISPR/Cas9 technology (38) to generate an E23K point mutation in the single exon of the *Kcnj11* gene (Fig. 1A). This method has the advantage that the Kir6.2-K23 variant is expressed from the endogenous promoter and gene locus, and no additional, potentially confounding, genetic elements are introduced. Thus, physiologically regulated gene expression is ensured. In our mouse, the E23 and K23 alleles differ by only two nucleotides: one in codon 23, which causes the E23K amino acid exchange, and a second, silent, mutation in codon 20 that creates a new *Bam*HI restriction enzyme cutting site. The latter was introduced to facilitate allele identification. Successful generation of the K23 allele was confirmed by PCR and sequencing (Fig. 1A), by copy number PCR, and by PCR and restriction digestion.

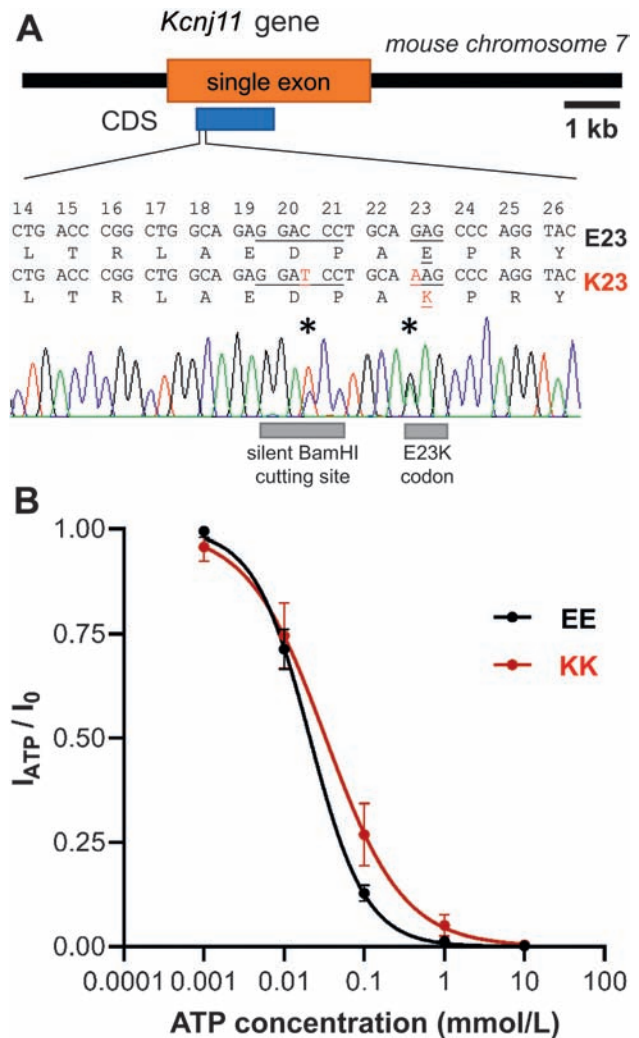


**Figure 1**—Generation and electrophysiological effect of the *Kcnj11*-K23 allele. **A**: Schematic of the *Kcnj11*-K23 allele, generated from the *Kcnj11*-E23 allele by CRISPR-assisted point mutagenesis. CDS is the coding sequence for the K<sub>ATP</sub> channel subunit Kir6.2. Codons for residues 14–26 of the E23 allele are shown, with the K23 allele below (point mutations are marked in red). Sequences for a silent *Bam*HI cutting site and the E23K codon are underlined. A DNA sequencing trace of a heterozygous E23K animal is shown at the bottom (C: blue, A: green, G: black, T: red), with the point mutations marked with asterisks (\*). **B**: Concentration-response curves for K<sub>ATP</sub> current inhibition by MgATP measured in inside-out patches from β-cells isolated from EE and KK mice. Current amplitude at a given MgATP concentration (*I*<sub>ATP</sub>) is expressed as a fraction of that in MgATP-free solution (*I*<sub>0</sub>). KK, *n* = 13 patches, *N* = 3 mice. EE, *n* = 18 patches, *N* = 4 mice. Heterozygous EK animals were excluded because of the small phenotypic effect expected for this group. Concentration-inhibition curves were individually fit with a Hill equation ( $y = a + (1 - a)/(1 + ([x]/IC_{50})^n)$ ) to determine IC<sub>50</sub> values. Lines represent Hill fits to all the individual data. Symbols show arithmetic mean and error bars the SEM. Some error bars are smaller than the symbol. Underlying data are available online (DOI: 10.6084/m9.figshare.12272873).

### Electrophysiological Effects in Mouse Isolated β-Cells

Our mouse model enabled us to study the effect of the Kir6.2-K23 variant in the β-cell, expressed under its native promoter and in its native cellular environment. We

isolated  $\beta$ -cells from mice with two K23 (KK) or two E23 (EE) alleles and measured the sensitivity of the  $K_{ATP}$ -channel to MgATP inhibition in inside-out membrane patches (Fig. 1B). The difference between the  $IC_{50}$  for MgATP inhibition in EE and of KK  $\beta$ -cells was not statistically significant ( $IC_{50} = 83 \pm 37 \mu\text{mol/L}$  [KK] and  $IC_{50} = 25 \pm 3 \mu\text{mol/L}$  [EE],  $P = \text{n.s.}$ , Welch  $t$  test). However, the extent of block at 100  $\mu\text{mol/L}$  MgATP was significantly reduced, the fractional current remaining being  $0.27 \pm 0.06$  ( $n = 13$ ) for KK  $\beta$ -cells compared with  $0.13 \pm 0.02$  ( $n = 13$ ) for EE  $\beta$ -cells ( $P = 0.046$ ).

### Blood Glucose Control on an SD

On the SD (RM3; Special Diets Services; Dietex), there was no difference in average body weight or body weight gain between EE and KK mice during the first 18 weeks of life (Fig. 2A), for either sex. Fed and fasting blood glucose levels were also similar in all groups (Figs. 2B and 3A). The time course of blood glucose changes during an IPGTT and the area under the curve (AUC) are shown for male and female EE and KK mice in Fig. 3A. There was a significant effect of both genotype ( $\Delta_{\text{geno}} = 288 \text{ min} \times \text{mmol/L}$ ,  $P = 0.005$ ) and sex ( $\Delta_{\text{sex}} = 1,228 \text{ min} \times \text{mmol/L}$ ,  $P < 0.0001$ ) on the AUC (mixed-model two-way ANOVA): male sex and

the KK genotype reduced glycemic control compared with female sex and the EE genotype.

To determine whether the elevated glucose during the IPGTT reflects reduced insulin release or decreased insulin sensitivity in KK animals, we performed an IPITT on 16-week-old mice (Fig. 3B). Note that because the insulin dose had to be adjusted for sex to avoid hypoglycemia, the data for male and female animals cannot be compared directly. The results suggest that insulin sensitivity was largely unaltered in both female and male KK mice. Thus, the IPITT data indicate that impaired glucose tolerance in KK mice was not caused by a decrease in insulin sensitivity. However, we cannot exclude the possibility that insulin sensitivity was slightly increased in male KK mice, as indicated by an increase of the AUC which was almost significant (EE:  $19.1 \pm 2.4\% \times \text{min}$ , KK:  $25.4 \pm 2.0\% \times \text{min}$ ,  $P = 0.06$ ).

In contrast, plasma insulin concentrations measured during IPGTTs revealed that impaired glucose tolerance correlated with reduced glucose-dependant insulin secretion in KK mice. Plasma insulin was not significantly different between KK and EE mice when considered independently of blood glucose (Fig. 3C). However, after the ratio between the plasma insulin AUC and the blood

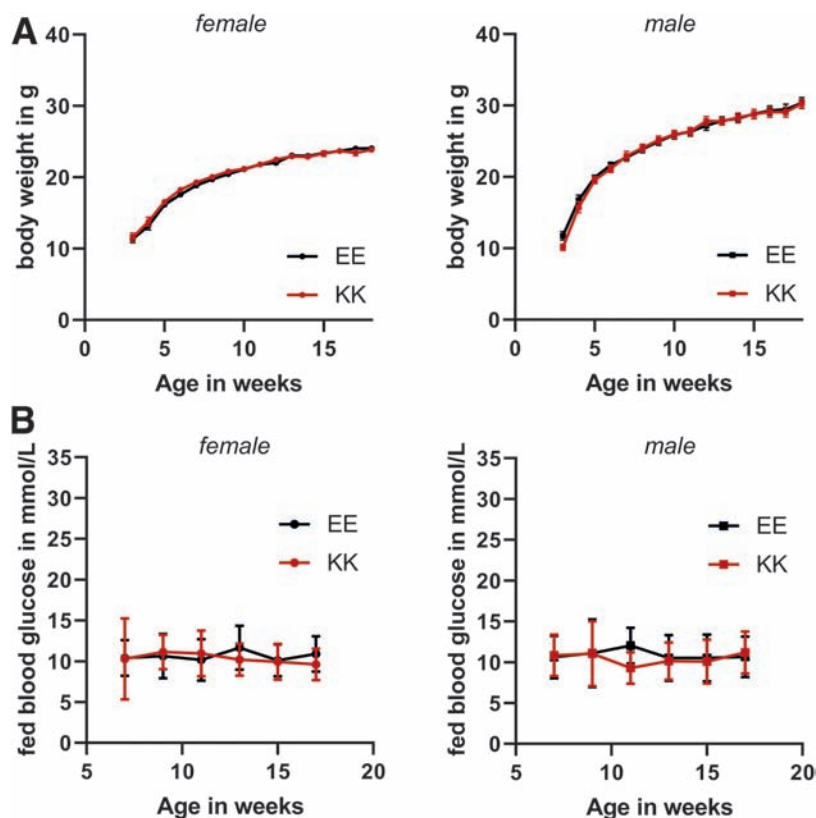


**Figure 2**—Body weight and fed blood glucose on the SD. *A*: Mean body weight of female and male animals carrying two risk alleles (KK) or none (EE), from 3 to 18 weeks of age. Error bars = SEM. Some error bars are smaller than the symbol. *B*: Mean fed blood glucose concentration of female and male KK mice and EE controls, from 7 to 17 weeks of age. Error bars = SD. Number of mice: female EE,  $N = 21$ ; female KK,  $N = 15$ ; male EE,  $N = 18$ ; male KK,  $N = 14$ . Underlying data are available online (DOI: 10.6084/m9.figshare.12272873).

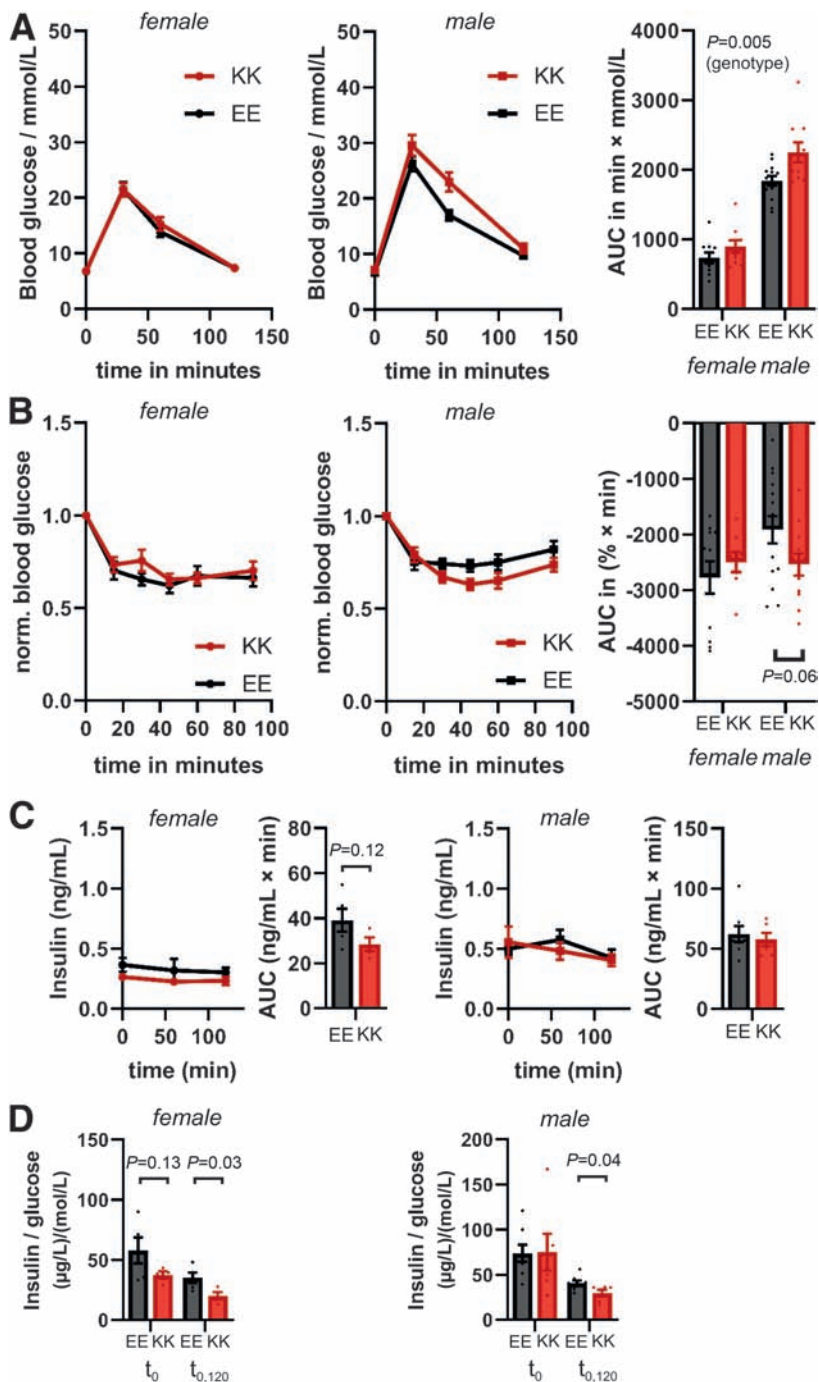


**Figure 3**—Glucose and insulin sensitivity on the SD. **A:** IPGTT for female (left) and male (middle) mice carrying two risk alleles (KK) or none (EE), at 12 weeks of age. Right, AUC. Statistical significance was analyzed using a mixed-model two-way ANOVA:  $P = 0.005$  (genotype),  $P < 0.0001$  (sex); no significant sex-genotype interaction. Number of mice: female EE,  $N = 10$ ; male EE,  $N = 13$ ; female KK,  $N = 10$ . **B:** IPITT for female (left) and male (middle) EE and KK mice at 16 weeks of age. Right, AUC below baseline (normalized 4-h fasted glucose). In male mice, the AUC (in %  $\times$  min) increased from  $1,913 \pm 244$  for EE mice to  $2,540 \pm 197$  for KK mice ( $P = 0.06$ , Welch  $t$  test). Number of mice: female EE,  $N = 11$ ; female KK,  $N = 9$ ; male EE,  $N = 15$ ; male KK,  $N = 12$ . The analysis excluded animals that showed no glucose response to the insulin injection (one female EE, two female KK, two male KK, and three male EE). Insulin dose was adjusted to  $0.75 \text{ IU/kg}_{\text{BW}}$  for female mice and  $1.0 \text{ IU/kg}_{\text{BW}}$  for male mice to minimize risk of hypoglycemia. **C:** Plasma insulin concentrations measured during the IPGTT for female and male EE and KK mice. Mean AUCs are shown to the right of traces. Number of mice: female EE,  $N = 5$ ; female KK,  $N = 4$ ; male EE,  $N = 8$ ; male KK,  $N = 6$ . The Welch  $t$  test was used to test for statistically significant differences. **D:** Mean plasma insulin-to-blood glucose ratios during the IPGTT for female and male EE and KK mice. Number of mice: female EE,  $N = 5$ ; female KK,  $N = 4$ ; male EE,  $N = 8$ ; male KK,  $N = 6$ .  $t_0$  denotes the overnight fasted state, preinjection. Insulin-to-glucose ratios were calculated by dividing insulin concentrations ( $t_0$ ) or AUC ( $t_{0,120}$ ) by their corresponding blood glucose values for each animal. Data were then averaged. Female insulin-to-glucose ( $t_{0,120}$ ): EE,  $35.1 \pm 4.3 \text{ (}\mu\text{g/L)/(mol/L)}$ ; KK,  $20.1 \pm 3.1 \text{ (}\mu\text{g/L)/(mol/L)}$  ( $P = 0.03$ ). Male insulin-to-glucose ( $t_{0,120}$ ): EE,  $40.6 \pm 2.8 \text{ (}\mu\text{g/L)/(mol/L)}$ ; KK,  $29.5 \pm 3.7 \text{ (}\mu\text{g/L)/(mol/L)}$  ( $P = 0.04$ ). The Welch  $t$  test was used to test for statistically significant differences. Data points correspond to individual animals. Error bars = SEM. Some error bars are smaller than the symbol. Underlying data are available online (DOI: 10.6084/m9.figshare.12272873).

glucose AUC ( $AUC_{ins-to-glu}$ ) for each individual animal was calculated, male and female KK mice both had significantly reduced insulin-to-glucose ratios (Fig. 3D). Preinjection ( $t_0$ ) insulin-to-glucose ratios were not significantly different. An alternative form of analysis, which involved plotting plasma insulin concentration as a function of blood glucose concentration for each individual animal and then fitting the insulin-glucose relationship by linear regression (Supplementary Fig. 1A), yielded equivalent results. Best-fit analysis revealed that after the glucose injection, KK mice secreted less insulin than their EE counterparts at a given blood glucose concentration. This was reflected by a significant change in the slope ( $\Delta_{ins}/\Delta_{glu}$ ) of the linear fits (Supplementary Fig. 1B).

### GSIS From Isolated Pancreatic Islets

Next, we examined insulin secretion in isolated pancreatic islets from EE and KK animals by batch incubation at low (2 mmol/L), intermediate (5–7 mmol/L), and high (20 mmol/L) glucose concentrations, and at 20 mmol/L glucose plus 10  $\mu$ mol/L glibenclamide to induce maximal  $K_{ATP}$  channel inhibition. Data were normalized to insulin content (Fig. 4A), which did not differ between experimental groups (Fig. 4B). Basal insulin secretion (2 mmol/L glucose) and maximal secretion (20 mmol/L glucose) did not differ between genotypes. However, insulin secretion at glucose concentrations around the threshold was impaired in KK islets ( $0.24 \pm 0.14$  % $_{total}/h$ ), which secreted only 39% as much insulin as EE islets ( $0.62 \pm 0.14$  % $_{total}/h$ ) at 7 mmol/L glucose ( $P = 0.01$ , mixed-model two-way ANOVA). Although the data for 5 mmol/L glucose are few, the trend is the same as for 7 mmol/L glucose. This effect was seen for both male and female KK mice and indicates that metabolism-secretion coupling is impaired at threshold glucose levels.

### Blood Glucose Control on an HFD

Because an HFD predisposes to obesity and diabetes, we next challenged mice with the HFD from 8 weeks of age and monitored their progression toward the diabetic state (Supplementary Material Part 1). As expected, all experimental groups gained more body weight on the HFD than on the SD. Weight gain on the HFD did not differ between female EE and KK mice, but male EE mice showed significantly more weight gain over time than their KK littermates (Fig. 5).

No animals developed uncontrolled diabetes (continuous-fed blood glucose levels  $>20$  mmol/L) during the study. However, there was a trend toward an increase in the fed blood glucose concentration (Supplementary Fig. 2), although data variability was too high to discern group differences. To gauge the magnitude of the HFD effect, we combined measurements for all animals that completed the phenotyping pipeline up to week 27 ( $N = 33$ ). For the pooled data, fed blood glucose concentrations (mean  $\pm$  SEM) were  $10.6 \pm 0.5$  mmol/L at week 7,  $12.2 \pm 0.4$  mmol/L at week 17 ( $P = 0.009$ , paired  $t$  test), and  $12.4 \pm 0.5$  mmol/L at week 27 ( $P = 0.004$ ). There was a comparable increase in fasted blood glucose, and measurements were less variable (Supplementary Table 1). Mean fasted blood glucose concentrations increased significantly on the HFD for female KK mice and for male KK and EE mice, but the change for female EE mice was not statistically significant (compare 4 weeks vs. 18 weeks on the HFD).

After the first 4 weeks on the HFD, at 12 weeks of age, male and female EE and KK mice both showed worse glycemic control than those fed the SD (Supplementary Fig. 3A). Insulin sensitivity, tested by IPITT at 16 weeks of age, was unchanged (Fig. 6A). Data from IPGTT at 12 weeks and IPITT at 16 weeks showed high variability, and

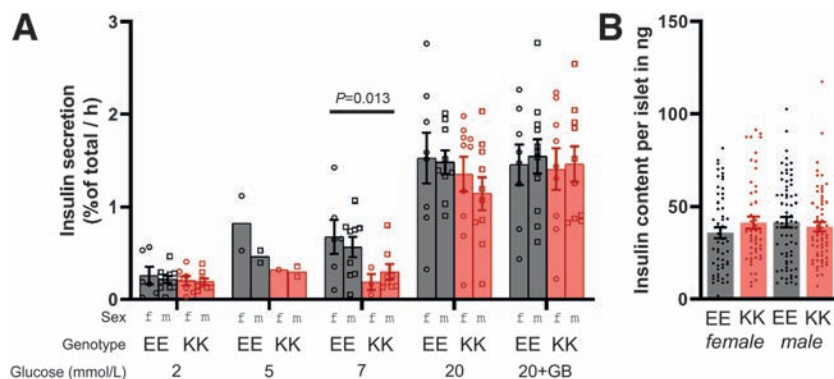


**Figure 4**—GSIS from pancreatic islets isolated from EE and KK mice fed the SD. A: Insulin secretion from islets was measured by batch incubation. GB = 10  $\mu$ mol/L glibenclamide. Individual batch secretion data were normalized to respective batch insulin content. Data points correspond to individual animals. The genotype effect at 7 mmol/L glucose was  $\Delta_{geno} = 0.38 \pm 0.14$  % $_{total}/h$ , ( $P = 0.013$ , mixed-model two-way ANOVA); whereas mouse sex had no effect ( $\Delta_{sex} = 0.00 \pm 0.14$  % $_{total}/h$ ,  $P = n.s.$ ). B: Mean islet insulin content, measured in batches. Data points correspond to individual batches. Number of batches ( $n$ ) and animals ( $N$ ): female EE,  $n = 54$ ,  $N = 11$ ; female KK,  $n = 50$ ,  $N = 10$ ; male EE,  $n = 69$ ,  $N = 12$ ; male KK,  $n = 63$ ,  $N = 10$ . Error bars = SEM. Underlying data are available online (DOI: 10.6084/m9.figshare.12272873).

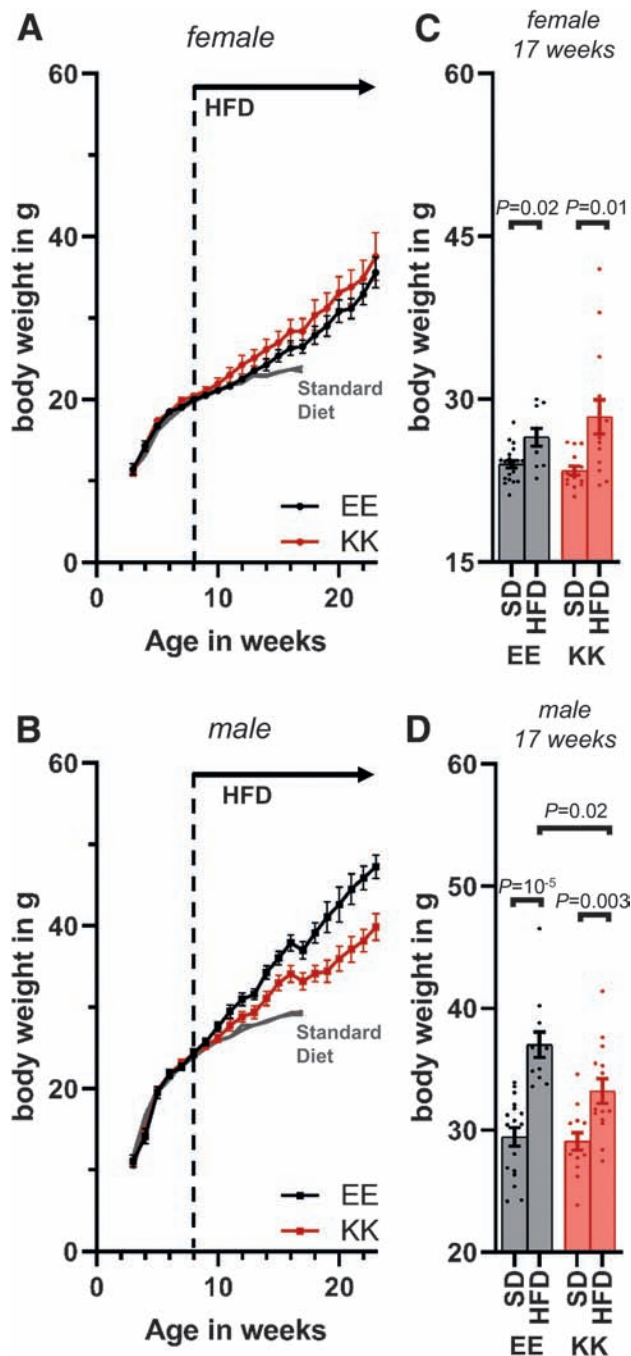


**Figure 5**—Body weight gain on the HFD. Average body weight for female (A) and male (B) EE and KK mice from 3 to 23 weeks of age. At 8 weeks of age (indicated by vertical dashed line), animals were switched from the SD to the HFD. SD: the mean weight of mouse cohorts that were not switched to the HFD is shown for comparison. Mean body weight of female (C) and male (D) EE and KK mice at 17 weeks of age fed the SD and HFD. The increase in weight was statistically significant for each group (Welch *t* test). Data points correspond to individual animals. Number of mice: female EE,  $N = 11$ ; female KK,  $N = 14$ ; male EE,  $N = 11$ ; male KK,  $N = 14$ . Error bars = SEM. Underlying data are available online (DOI: 10.6084/m9.figshare.12420839).

genotype differences were not statistically significant, except for male KK mice, which secreted significantly less insulin ( $93 \pm 11$  ng/mL) than their EE counterparts during an IPGTT ( $145 \pm 21$  ng/mL;  $P = 0.04$ , Welch

*t* test) (Supplementary Fig. 3B), even when adjusted for blood glucose concentration (Supplementary Figs. 3C and 4).

Glucose tolerance tests at 26 weeks of age, after 18 weeks on the HFD, showed substantially reduced glycemic control for both sexes and all genotypes (Fig. 6B). Female KK mice were significantly more impaired than EE mice, and the AUC was increased (EE,  $1.8 \pm 0.2$  min  $\times$  mol/L; KK,  $2.5 \pm 0.3$  min  $\times$  mol/L;  $P = 0.04$ , Welch *t* test). Glycemic control was very poor in male mice, such that the mean blood glucose remained  $\sim 30$  mmol/L even 120 min after injection, for both genotypes (Fig. 6B). Insulin responses during an IPGTT varied tremendously for female KK mice, with two individuals showing very high insulin secretion, while most other female KK mice secreted less insulin at a given glucose concentration than their EE counterparts. This affected the mean of both the plasma insulin concentration (Fig. 6C) and the insulin-to-glucose ratio (Fig. 6D and Supplementary Fig. 5), and no statistically significant genotype differences could be detected for female mice. However, male KK mice secreted significantly less insulin during an IPGTT than male EE mice, both in the fasting state ( $t_0$ ) and after glucose injection ( $t_{0,120}$ ) (Fig. 6C). As a consequence, their mean insulin-to-glucose ratios were about half as large as the mean ratios for male EE mice, both when calculated from the AUC ratios (Fig. 6D) or when determined by scatter plot linear regression (Supplementary Fig. 5).

Additionally, we measured postmortem levels of HbA<sub>1c</sub>, which provides an indication of the integrated blood glucose level during the preceding month (the half-life of a mouse red blood cell is  $\sim 23$  days; [41]). In addition to EE and KK mice, we also used  $\beta$ -V59M mice (42), in which diabetes can be induced, as technical controls for the assay. Diabetic  $\beta$ -V59M mice were kept for 14 days after induction (fed blood glucose  $>44$  mmol/L) before blood sampling alongside their nondiabetic littermates (Fig. 7). The mean HbA<sub>1c</sub> level was  $8.0 \pm 0.5\%$  ( $64 \pm 5$  mmol/mol) in diabetic mice ( $N = 5$ ), substantially higher than that of  $5.2 \pm 0.3\%$  ( $33 \pm 3$  mmol/mol) in nondiabetic mice ( $N = 5$ ). Values for 28-week-old EE and KK mice, which had been maintained on the HFD for 20 weeks, lay between these values.

#### GSIS From Isolated Pancreatic Islets

We next measured GSIS from pancreatic islets isolated from EE and KK animals at 23 weeks of age (15 weeks on the HFD). Notably, GSIS from male (but not female) KK islets was severely reduced at all glucose concentrations (Fig. 8A). This correlated with a reduction in insulin content in male KK islets, which was  $\sim 45\%$  lower than in the other HFD experimental groups, including male EE mice (Fig. 8B). However, the low insulin content could not fully account for the loss of insulin secretion seen in male KK islets. We also plotted insulin release at 20 mmol/L glucose + glibenclamide as a fraction of the insulin content to determine whether stimulus-secretion coupling was impaired (Fig. 8C). Content-normalized secretion was

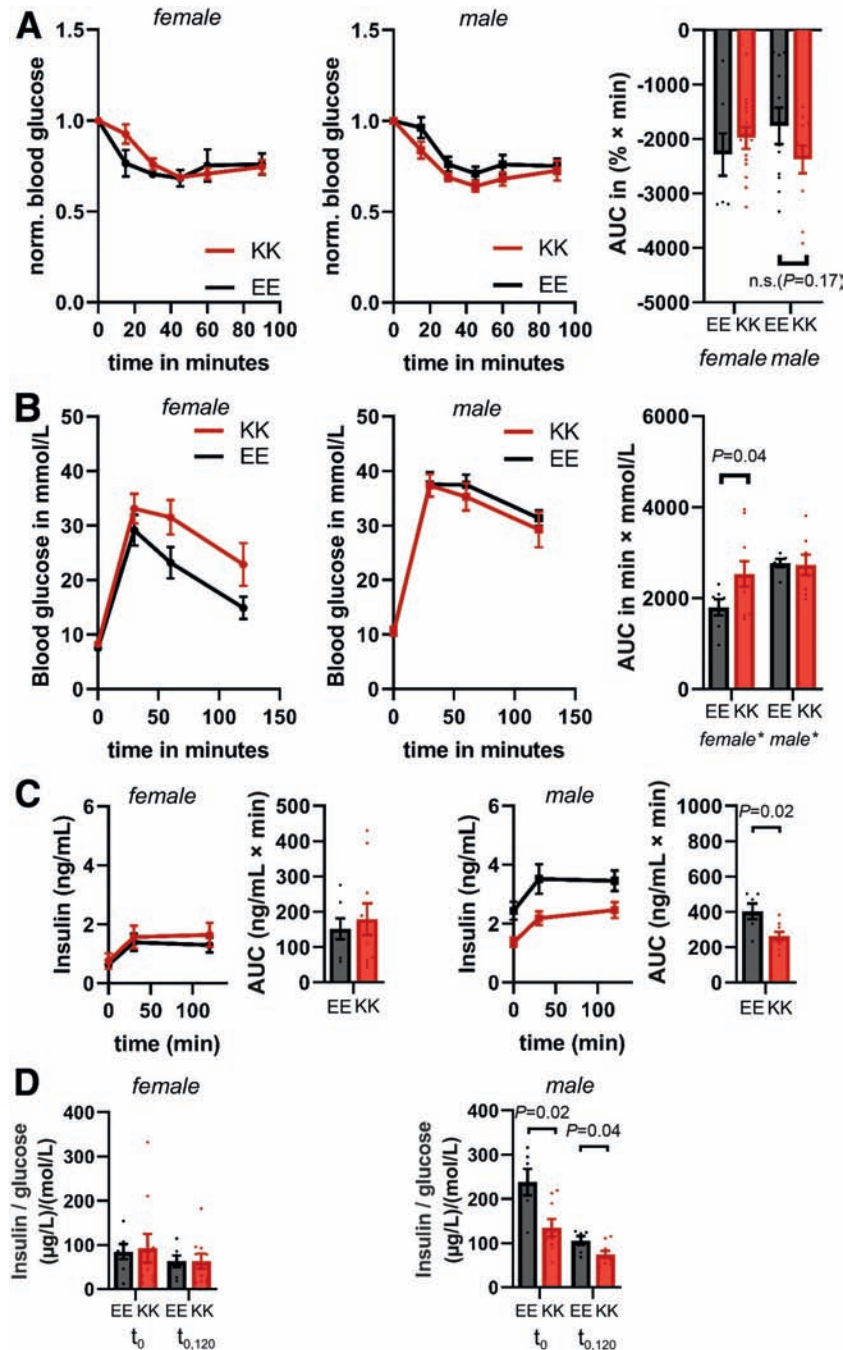


**Figure 6**—Insulin and glucose sensitivity on the HFD. **A:** IPITT for female (left) and male (middle) EE and KK mice fed the HFD at 16 weeks of age. Right, AUC. Number of mice: female EE,  $N = 7$ ; female KK,  $N = 14$ ; male EE,  $N = 11$ ; male KK,  $N = 11$ . Animals that showed no glucose response to insulin injection (three female EE, one male EE, three male KK) were excluded from the analysis. Because the insulin dose had to be adjusted for sex to avoid hypoglycemia, IPITT curves for male and female mice are not directly comparable. **B:** IPGTT for female (left) and male (middle) mice carrying two risk alleles (KK) or none (EE) at 26 weeks of age (HFD from 8 weeks of age). Right, AUC. Number of mice: female EE,  $N = 7$ ; female KK,  $N = 10$ ; male EE,  $N = 6$ ; male KK,  $N = 9$ . \*Some data points reached the upper detection limit of 44 mmol/L, affecting traces of five female KK, two male EE, and three male KK mice. Genotype effects were not statistically significant in mixed-model two-way ANOVA, but the AUC of female KK mice was significantly increased compared with EE when considered separately (EE  $1.8 \pm 0.2$  min  $\times$  mol/L, KK  $2.5 \pm 0.3$  min  $\times$  mol/L;  $P = 0.04$ , Welch  $t$  test). **C:** Plasma insulin concentrations measured during the IPGTT for female and male EE and KK mice. Number of mice: female EE,  $N = 7$ ; female KK,  $N = 10$ ; male EE,  $N = 6$ ; male KK,  $N = 9$ . AUCs are shown to the right of traces. Insulin secretion was significantly reduced for male KK mice (EE,  $403 \pm 44$  ng/h/mL; KK,  $262 \pm 24$  ng/h/mL;  $P = 0.02$ , Welch  $t$  test). **D:** Mean plasma insulin-to-blood glucose ratios during the IPGTT shown in **B** for female and male EE and KK mice.  $t_0$  denotes the overnight fasted state, preinjection. Ratios were calculated by dividing insulin concentrations ( $t_0$ ) or AUC ( $t_{0,120}$ ) by their corresponding blood glucose values for each animal. Data were then averaged. Data points shown correspond to individual animals. Number of mice: female EE,  $N = 7$ ; female KK,  $N = 10$ ; male EE,  $N = 6$ ; male KK,  $N = 9$ . Ratios were reduced for male KK animals at  $t_0$  (EE,  $238 \pm 30$  ( $\mu\text{g/L})/(\text{mol/L})$ ; KK,  $135 \pm 19$  ( $\mu\text{g/L})/(\text{mol/L})$ ;  $P = 0.02$ , Welch  $t$  test) and for the AUC (EE,  $106 \pm 10$  ( $\mu\text{g/L})/(\text{mol/L})$ ; KK,  $74 \pm 8$  ( $\mu\text{g/L})/(\text{mol/L})$ ;  $P = 0.04$ , Welch  $t$  test). Data points correspond to individual animals. Error bars = SEM. Some error bars are smaller than the symbol. Underlying data are available online (DOI: 10.6084/m9.figshare.12420839).

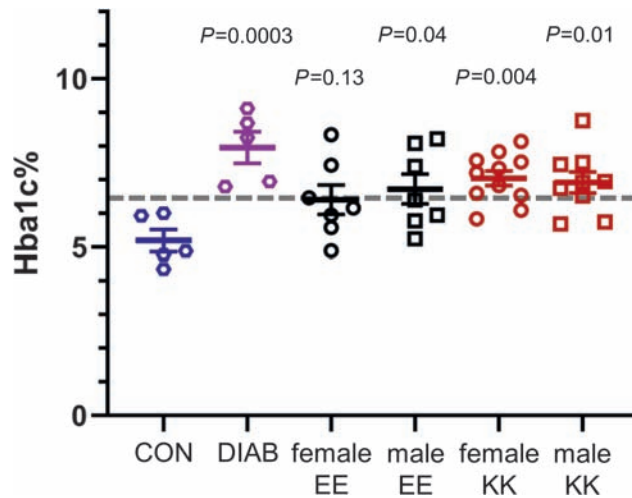


**Figure 7**—HbA<sub>1c</sub> at 28 weeks of age (HFD from week 8). Fraction of HbA<sub>1c</sub> in blood samples taken postmortem at 28 weeks of age.  $\beta$ -V59M mice with inducible diabetes served as technical controls. Here, blood samples were taken 2 weeks after induction of severe diabetes (>44 mmol/L blood glucose) in  $\beta$ -V59M mice (DIAB), or from normoglycemic littermates (CON). Mean  $\pm$  SEM and individual data points are shown. Female EE:  $6.4 \pm 0.4\%$  ( $46 \pm 4$  mmol/mol),  $N = 7$ ; female KK:  $7.0 \pm 0.2\%$  ( $53 \pm 2$  mmol/mol),  $N = 11$ ; male EE:  $6.7 \pm 0.4\%$  ( $50 \pm 4$  mmol/mol),  $N = 7$ ; male KK:  $6.9 \pm 0.4\%$  ( $52 \pm 4$  mmol/mol),  $N = 9$ . The dotted line denotes the middle value between the DIAB ( $8.0 \pm 0.5\%$  [ $64 \pm 5$  mmol/mol],  $N = 5$ ) and CON ( $5.2 \pm 0.3\%$  [ $33 \pm 3$  mmol/mol],  $N = 5$ ) groups.  $P$  values shown are for comparison with the nondiabetic control group (CON) and were adjusted for post hoc multiple comparison with the Dunnett test. Note the background strain is different for the experimental EE and KK mice (C57BL/6NTac) than for control and diabetic  $\beta$ -V59M mice (C57BL/6J). Error bars = SEM. Underlying data are available online (DOI: 10.6084/m9.figshare.12420839).

substantially lower in islets from both male EE (40% remaining) and KK mice (24% remaining) on the HFD. This suggests a decline in  $\beta$ -cell function that is characterized by reduced insulin content and impaired stimulus-secretion coupling.

## DISCUSSION

The effect of the E23K polymorphism on  $K_{ATP}$  channel function has long been controversial. Our results are the first characterization of the Kir6.2-K23 variant in pancreatic  $\beta$ -cells and expressed under its native promoter (previous studies were confined to recombinant channels heterologously expressed in cell lines or *Xenopus* oocytes). The results suggest that the Kir6.2-K23 subunit confers a slight, and therefore, hard-to-detect reduction in sensitivity to inhibition by MgATP compared with its E23 counterpart (Fig. 1B). Because insulin secretion *in vivo* is regulated at glucose levels at which the  $K_{ATP}$  channel is almost totally inhibited, small changes in  $K_{ATP}$  current at these threshold concentrations (5–7 mmol/L) have a dramatic effect on membrane potential and electrical activity. Thus, insulin secretion is exquisitely sensitive to the  $K_{ATP}$  current magnitude at these concentrations, and a very

small decrease in current has the potential to significantly shift the insulin concentration-response curve to glucose. This is consistent with the reduced insulin secretion seen in isolated islets at 7 mmol/L glucose (Fig. 4A). Our data agree with a spectrum of previous studies, which report a small gain-of-function (22,30,31), no change (32,34), or a statistically insignificant decrease in ATP inhibition (33). Moreover, a small shift in the concentration dependence of ATP inhibition is the best explanation for our finding that isolated pancreatic islets with the KK genotype secrete less insulin than EE islets at intermediate (5–7 mmol/L), but not at high (20 mmol/L) or low (2 mmol/L) glucose concentrations (Fig. 4A). Importantly, this effect was observed in islets from both male and female mice.

When fed the SD, KK mice exhibited reduced systemic insulin secretion in response to glucose injection (Fig. 3D and Supplementary Fig. 2), resulting in slightly impaired glycemic control (Fig. 3A). Although we found no statistically significant genotype-sex interaction, this effect was more obvious in male mice. There was no effect on the fasting or the fed blood glucose concentration (Supplementary Table 1 and Fig. 2B). Our results resemble those of a human study that found the K23 risk allele was associated with reduced systemic insulin secretion and a compensatory increase in insulin sensitivity, but no overall change in blood glucose concentrations (22). Because the variability of the IPITT data were too high to detect a statistically significant difference (Fig. 3B), we cannot exclude the possibility that KK mice also have increased insulin sensitivity. Therefore, it might be worthwhile to investigate glycemic control and insulin sensitivity in KK animals at a later time point (after >6 months on the HFD), when phenotypes have stabilized.

Because the risk of T2D is exacerbated by an HFD and by obesity, we challenged EE and KK mice with the HFD from the age of 8 weeks. Consistently, the KK genotype, male sex, and HFD duration were correlated with poorer outcomes, whereas the EE genotype, female sex, and the SD were protective. However, in some experiments, a combination of two or more factors was required to produce a significant effect. For example,  $\beta$ -cell failure occurred in islets of male mice with the KK genotype after 15 weeks on the HFD, but not in female KK or male EE mice (Fig. 8). Analogously, female EE mice on the HFD appeared to be protected from an increase in fasted blood glucose levels, whereas blood glucose rose in female KK and male EE mice (Supplementary Table 1). In some experiments, we observed trends that were consistent with the risk factors mentioned above, but which would require unfeasible statistical power ( $N > 200$ ) to determine whether they were statistically significant (Figs. 7 and 8B and C). Overall, differences in glycemic control between EE and KK genotypes were harder to detect in female mice (Figs. 3 and 6D). However, sex did not influence genotype effects on insulin secretion at threshold glucose concentrations (Fig. 4). To date, several hundred thousand case and control subjects have been analyzed in >90 genome-wide

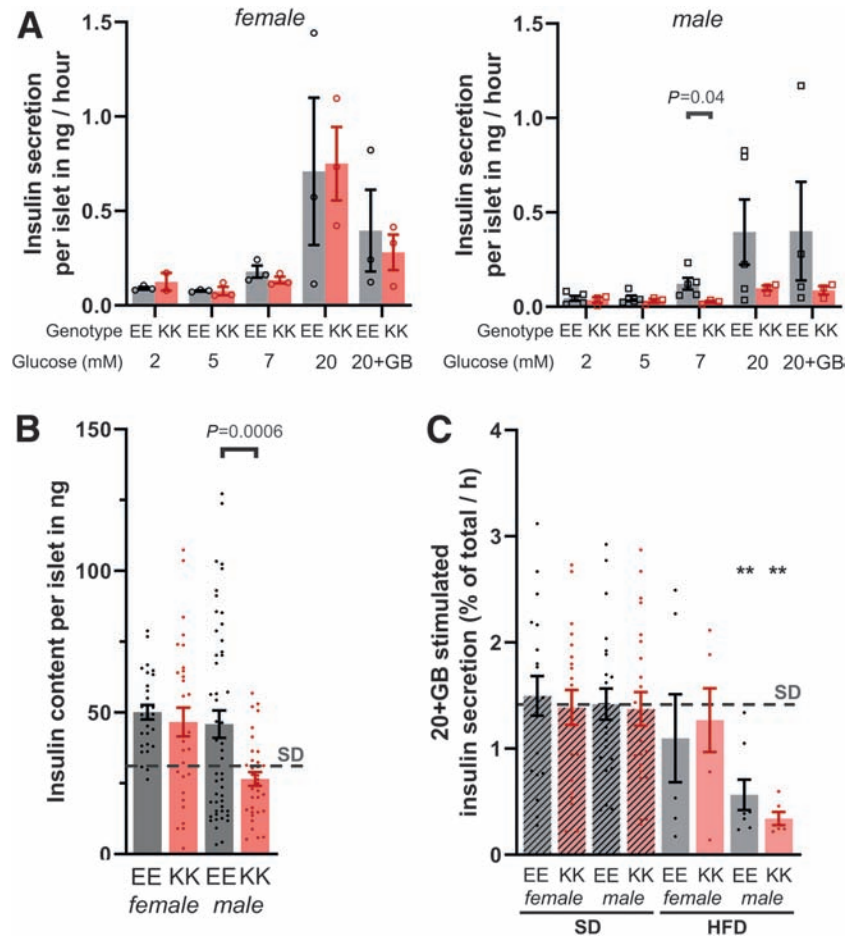


**Figure 8**—GSIS from pancreatic islets isolated from EE and KK mice at 23 weeks of age after 15 weeks on the HFD. Insulin secretion from islets was measured by batch incubation. GB = 10  $\mu$ mol/L glibenclamide. Mean  $\pm$  SEM and individual data points are shown. Underlying data are available online (DOI: 10.6084/m9.figshare.12420839). **A**: Mean insulin secretion per isolated islet per hour (not normalized to content). Data points correspond to individual animals (female EE,  $N = 3$ ; female KK,  $N = 3$ ; male EE,  $N = 5$ ; male KK,  $N = 4$ ). At 7 mmol/L: EE  $0.121 \pm 0.031$  ng/h/islet, KK  $0.026 \pm 0.006$  ng/h/islet;  $P = 0.037$  (Welch  $t$  test). **B**: Mean insulin content per islet for each experimental group. Data points correspond to individual batches. Overall SD average ( $39.6 \pm 1.4$  ng/islet,  $n = 236$ ) is marked by a horizontal dashed line. Number of batches ( $n$ ) and animals ( $N$ ): female EE,  $n = 29$ ,  $N = 3$ ; female KK,  $n = 30$ ,  $N = 3$ ; male EE,  $n = 50$ ,  $N = 5$ ; male KK,  $n = 34$ ,  $N = 4$ . Insulin content was significantly reduced in male KK mice ( $26.5 \pm 2.4$  ng/islet) compared with EE littermates ( $45.9 \pm 4.8$  ng/islet;  $P = 0.0006$ , Welch  $t$  test). **C**: Insulin secretion from isolated islets stimulated with 20 mmol/L glucose + GB and normalized to total insulin content for all experimental groups. Data points correspond to individual batches. Number of batches ( $n$ ) and animals ( $N$ ): SD female EE,  $n = 19$ ,  $N = 12$ ; SD female KK,  $n = 21$ ,  $N = 10$ ; SD male EE,  $n = 23$ ,  $N = 11$ ; SD male KK,  $n = 23$ ,  $N = 20$ ; HFD female EE,  $n = 6$ ,  $N = 3$ ; HFD female KK,  $n = 6$ ,  $N = 3$ ; HFD male EE,  $n = 8$ ,  $N = 5$ ; HFD male KK,  $n = 6$ ,  $N = 3$ . \*\*Male EE:  $0.57 \pm 0.14$  % $_{\text{total}}/h$ ,  $P = 0.008$ ; male KK:  $0.34 \pm 0.06$  % $_{\text{total}}/h$ ,  $P = 0.003$ ; one-way ANOVA, Dunnett test with SD overall average ( $1.42 \pm 0.08$  % $_{\text{total}}/h$ ) as control (dotted line).

association studies (1), but except for one small-scale study with mixed results (43), no sex-specific effects of the E23K variant have been reported. In addition to enhancing T2D risk, the E23K polymorphism has also been found to increase the risk of gestational diabetes (44).

Our data show that a small reduction in the glucose sensitivity of insulin secretion, such as that conferred by the E23K mutation, has only a small effect on glycemic control when animals are maintained on the SD (Fig. 3). However, the HFD (and/or the accompanying obesity), together with the KK genotype, causes impairment of glucose tolerance in female mice (Fig. 6B) and markedly reduced glucose-induced insulin secretion in male mice (Fig. 8). The extent of glucose intolerance in male mice

could not be reliably determined because of off-scale glucose readings in some animals (Fig. 6B). Our data indicate that even mild impairment of  $\beta$ -cell function may cause loss of glycemic control in response to stress, such as that imposed by an HFD. The resulting incremental hyperglycemia causes further impairment of  $\beta$ -cell function, leading to a vicious cycle in which rising blood glucose exacerbates  $\beta$ -cell failure leading to a further increase in hyperglycemia (45,46).

It is noteworthy that on the SD, male KK mouse islets secreted less insulin at glucose concentrations around threshold (7 mmol/L) than EE islets (Fig. 4). However, on the HFD, insulin secretion was impaired at all glucose concentrations (Fig. 8A). This was, at least partly caused by a failure to increase their insulin content in response to the

increased demand (Fig. 8B). It is important to recognize, however, that a decrease in insulin content does not necessarily translate into a parallel reduction in insulin secretion. Only a tiny proportion of the insulin granules in the cell—those docked at the plasma membrane—are released in response to elevation of blood glucose. It is quite possible that the number of docked granules is unaffected in KK mice. It is likely that stimulus-secretion coupling is also affected given the reduced ATP sensitivity of the  $K_{ATP}$  channel in KK mice—indeed, this must be the case initially. Experiments on mice carrying more severe  $K_{ATP}$  channel mutations suggest that a loss of insulin content and impaired insulin stimulus-secretion coupling are both involved (46,47). Our data also support the finding that in human T2D,  $\beta$ -cell function declines substantially (by ~50%) before diabetes diagnosis (48).

Our data suggest that the E23K polymorphism is important early in the development of diabetes and underlies the initial loss of glycemic control. This is in agreement with two genome-wide association studies that found a strong effect of the E23K polymorphism on the transition from normal glucose tolerance to prediabetes, but little effect on the progression from impaired glucose tolerance to full diabetes (4,21). Thus, the E23K risk effect may have been significantly underestimated in some studies, depending on whether the examined cohort had mostly healthy or already impaired glycemic control at the time of study. This can therefore at least partly explain why reported ORs for the E23K polymorphism vary from 1.0 to 1.7 between studies (1). Our findings have implications for risk-allele-specific personalized diabetes treatment. They emphasize it is particularly advisable for individuals with the KK genotype to avoid weight gain and maintain good glycemic control to reduce their chance of progression to diabetes. It would therefore be of interest to determine whether early lifestyle intervention and weight loss are indeed especially beneficial for KK carriers. The KK genotype has been linked to an increased likelihood of secondary failure of sulfonylurea treatment (49), which can result from an increased decline of  $\beta$ -cell function (50).

In summary, we conclude that the *KCNJ11-K23* variant alone is sufficient to increase diabetes risk. This does not, of course, exclude a role of other gene variants (e.g., *ABCC8-S1369A*). Our results also help to explain how the K23 allele increases diabetes risk. It does so by producing a small decrease in  $K_{ATP}$  channel inhibition by  $MgATP$ , which causes a right-shift in the relationship between insulin secretion and glucose concentration. Consequently, the threshold for GSIS from islets is increased, and insulin release in response to glucose injections is reduced. When other risk factors are present (HFD/obesity), the deleterious effects of the KK genotype are exacerbated, leading to an earlier decrease of  $\beta$ -cell function. Chronic hyperglycemia further impairs insulin secretion, triggering a vicious cycle that fuels a progressive deterioration in  $\beta$ -cell function and conversion of impaired glucose tolerance to overt diabetes. The K23 allele mouse model

represents an important resource that will aid our understanding of the risk-allele-specific pathogenesis and inform future studies on K23-specific personalized diabetes treatment.

**Acknowledgments.** The authors thank Michelle Stewart (Harwell, Oxfordshire, U.K.) for facilitation, logistics, and method advice. The authors also thank Sara Wells and Lydia Teboul (Harwell, Oxfordshire, U.K.) and the staff at the Mary Lyon Centre (Harwell) for gene delivery, husbandry, phenotyping, molecular biology, and necropsy teams for excellent animal care and service. The C57BL/6NTac-Kcnj11<sup>em1H</sup>/H mice were obtained from the MRC Harwell Institute, which distributes these mice on behalf of the European Mouse Mutant Archive ([www.infrafrontier.eu](http://www.infrafrontier.eu)). The MRC Harwell Institute delivered the C57BL/6NTac-Kcnj11<sup>em1H</sup>/H mouse strain as part of its commitment to the Genome Editing Mice for Medicine project funded [MC\_UP\_1502/3] by the Medical Research Council.

The research reported in this publication is solely the responsibility of the authors and does not necessarily represent the official views of the Medical Research Council.

**Funding.** Support was received from the European Research Council (322620 to F.M.A.), the Medical Research Council (MR/T002107/1 to E.H. and F.M.A. and MC\_U142661184 to R.D.C.), the Biotechnology and Biological Research Council (BB/R017220/1 to G.S. and F.M.A.), and the Nuffield Benefaction for Medicine/Wellcome Institutional Strategic Support Fund (Oxford MSIF grant 0005155, to G.S.). F.M.A. held an European Research Council Advanced Investigatorship.

**Duality of Interest.** No potential conflicts of interest relevant to this article were reported.

**Author Contributions.** G.S., E.H., T.H., P.P., R.J., and R.T.-E. performed experiments. G.S., E.H., T.H., P.P., S.J.T., R.D.C., and F.M.A. reviewed and edited the manuscript. G.S., P.P., and R.J. analyzed the data. G.S., R.D.C., and F.M.A. designed the study. G.S. and F.M.A. wrote the manuscript. L.B. performed preliminary experiments and was involved in the animal logistics, planning, and organization. G.S. is the guarantor of this work and, as such, had full access to all the data in the study and takes responsibility for the integrity of the data and the accuracy of the data analysis.

## References

- Sokolova EA, Bondar IA, Shabelnikova OY, Pyankova OV, Filipenko ML. Replication of *KCNJ11* (p.E23K) and *ABCC8* (p.S1369A) association in Russian diabetes mellitus 2 type cohort and meta-analysis. *PLoS One* 2015;10:e0124662
- Sakura H, Wat N, Horton V, Millns H, Turner RC, Ashcroft FM. Sequence variations in the human *Kir6.2* gene, a subunit of the beta-cell ATP-sensitive K-channel: no association with NIDDM in white Caucasian subjects or evidence of abnormal function when expressed in vitro. *Diabetologia* 1996;39:1233–1236
- Gloyn AL, Weedon MN, Owen KR, et al. Large-scale association studies of variants in genes encoding the pancreatic beta-cell KATP channel subunits *Kir6.2* (*KCNJ11*) and *SUR1* (*ABCC8*) confirm that the *KCNJ11* E23K variant is associated with type 2 diabetes. *Diabetes* 2003;52:568–572
- Cheung CY, Tso AW, Cheung BM, et al. The *KCNJ11* E23K polymorphism and progression of glycaemia in Southern Chinese: a long-term prospective study. *PLoS One* 2011;6:e28598
- Mtiraoui N, Turki A, Nemr R, et al. Contribution of common variants of *ENPP1*, *IGF2BP2*, *KCNJ11*, *MLXIPL*, *PPAR $\gamma$* , *SLC30A8* and *TCF7L2* to the risk of type 2 diabetes in Lebanese and Tunisian Arabs. *Diabetes Metab* 2012;38:444–449
- Ashcroft FM, Harrison DE, Ashcroft SJ. Glucose induces closure of single potassium channels in isolated rat pancreatic beta-cells. *Nature* 1984;312:446–448
- Rorsman P, Ashcroft FM. Pancreatic  $\beta$ -cell electrical activity and insulin secretion: of mice and men. *Physiol Rev* 2018;98:117–214
- Gloyn AL, Pearson ER, Antcliff JF, et al. Activating mutations in the gene encoding the ATP-sensitive potassium-channel subunit *Kir6.2* and permanent neonatal diabetes. *N Engl J Med* 2004;350:1838–1849

9. Flanagan SE, Patch AM, Mackay DJ, et al. Mutations in ATP-sensitive K<sup>+</sup> channel genes cause transient neonatal diabetes and permanent diabetes in childhood or adulthood. *Diabetes* 2007;56:1930–1937
10. Edghill EL, Flanagan SE, Ellard S. Permanent neonatal diabetes due to activating mutations in *ABCC8* and *KCNJ11*. *Rev Endocr Metab Disord* 2010;11:193–198
11. De Franco E, Flanagan SE, Houghton JA, et al. The effect of early, comprehensive genomic testing on clinical care in neonatal diabetes: an international cohort study. *Lancet* 2015;386:957–963
12. Masia R, Koster JC, Tumini S, et al. An ATP-binding mutation (G334D) in *KCNJ11* is associated with a sulfonyleurea-insensitive form of developmental delay, epilepsy, and neonatal diabetes. *Diabetes* 2007;56:328–336
13. Babenko AP, Polak M, Cavé H, et al. Activating mutations in the *ABCC8* gene in neonatal diabetes mellitus. *N Engl J Med* 2006;355:456–466
14. Proks P, Girard C, Baevre H, Njølstad PR, Ashcroft FM. Functional effects of mutations at F35 in the NH<sub>2</sub>-terminus of Kir6.2 (*KCNJ11*), causing neonatal diabetes, and response to sulfonyleurea therapy. *Diabetes* 2006;55:1731–1737
15. Gloy AL, Reimann F, Girard C, et al. Relapsing diabetes can result from moderately activating mutations in *KCNJ11*. *Hum Mol Genet* 2005;14:925–934
16. McTaggart JS, Clark RH, Ashcroft FM. The role of the KATP channel in glucose homeostasis in health and disease: more than meets the islet. *J Physiol* 2010;588:3201–3209
17. D'Amato E, Tammaro P, Craig TJ, et al. Variable phenotypic spectrum of diabetes mellitus in a family carrying a novel *KCNJ11* gene mutation. *Diabet Med* 2008;25:651–656
18. Tarasov AI, Nicolson TJ, Riveline JP, et al. A rare mutation in *ABCC8/SUR1* leading to altered ATP-sensitive K<sup>+</sup> channel activity and beta-cell glucose sensing is associated with type 2 diabetes in adults. *Diabetes* 2008;57:1595–1604
19. Liu L, Nagashima K, Yasuda T, et al. Mutations in *KCNJ11* are associated with the development of autosomal dominant, early-onset type 2 diabetes. *Diabetologia* 2013;56:2609–2618
20. Hani EH, Boutin P, Durand E, et al. Missense mutations in the pancreatic islet beta cell inwardly rectifying K<sup>+</sup> channel gene (*KIR6.2/BIR*): a meta-analysis suggests a role in the polygenic basis of Type II diabetes mellitus in Caucasians. *Diabetologia* 1998;41:1511–1515
21. Florez JC, Jablonski KA, Kahn SE, et al. Type 2 diabetes-associated missense polymorphisms *KCNJ11* E23K and *ABCC8* A1369S influence progression to diabetes and response to interventions in the Diabetes Prevention Program. *Diabetes* 2007;56:531–536
22. Villareal DT, Koster JC, Robertson H, et al. Kir6.2 variant E23K increases ATP-sensitive K<sup>+</sup> channel activity and is associated with impaired insulin release and enhanced insulin sensitivity in adults with normal glucose tolerance. *Diabetes* 2009;58:1869–1878
23. Nielsen EM, Hansen L, Carstensen B, et al. The E23K variant of Kir6.2 associates with impaired post-OGTT serum insulin response and increased risk of type 2 diabetes. *Diabetes* 2003;52:573–577
24. Tschritter O, Stumvoll M, Machicao F, et al. The prevalent Glu23Lys polymorphism in the potassium inward rectifier 6.2 (*KIR6.2*) gene is associated with impaired glucagon suppression in response to hyperglycemia. *Diabetes* 2002;51:2854–2860
25. Hart LM, van Haefen TW, Dekker JM, Bot M, Heine RJ, Maassen JA. Variations in insulin secretion in carriers of the E23K variant in the *KIR6.2* subunit of the ATP-sensitive K<sup>+</sup> channel in the beta-cell. *Diabetes* 2002;51:3135–3138
26. Li N, Wu JX, Ding D, Cheng J, Gao N, Chen L. Structure of a pancreatic ATP-sensitive potassium channel. *Cell* 2017;168:101–110.e10
27. Lee KPK, Chen J, MacKinnon R. Molecular structure of human KATP in complex with ATP and ADP. *eLife* 2017;6:e32481
28. Martin GM, Kandasamy B, DiMaio F, Yoshioka C, Shyng SL. Anti-diabetic drug binding site in a mammalian K<sub>ATP</sub> channel revealed by Cryo-EM. *eLife* 2017;6:e31054
29. Martin GM, Yoshioka C, Rex EA, et al. Cryo-EM structure of the ATP-sensitive potassium channel illuminates mechanisms of assembly and gating. *eLife* 2017;6:e24149
30. Schwanstecher C, Meyer U, Schwanstecher M. K<sub>(IR)6.2</sub> polymorphism predisposes to type 2 diabetes by inducing overactivity of pancreatic beta-cell ATP-sensitive K<sup>+</sup> channels. *Diabetes* 2002;51:875–879
31. Schwanstecher C, Neugebauer B, Schulz M, Schwanstecher M. The common single nucleotide polymorphism E23K in K<sub>(IR)6.2</sub> sensitizes pancreatic beta-cell ATP-sensitive potassium channels toward activation through nucleoside diphosphates. *Diabetes* 2002;51(Suppl. 3):S363–S367
32. Riedel MJ, Boora P, Steckley D, de Vries G, Light PE. Kir6.2 polymorphisms sensitize beta-cell ATP-sensitive potassium channels to activation by acyl CoAs: a possible cellular mechanism for increased susceptibility to type 2 diabetes? *Diabetes* 2003;52:2630–2635
33. Vedovato N, Cliff E, Proks P, et al. Neonatal diabetes caused by a homozygous *KCNJ11* mutation demonstrates that tiny changes in ATP sensitivity markedly affect diabetes risk. *Diabetologia* 2016;59:1430–1436
34. Hamming KS, Soliman D, Matemiz LC, et al. Coexpression of the type 2 diabetes susceptibility gene variants *KCNJ11* E23K and *ABCC8* S1369A alter the ATP and sulfonyleurea sensitivities of the ATP-sensitive K<sup>+</sup> channel. *Diabetes* 2009;58:2419–2424
35. Florez JC, Burt N, de Bakker PI, et al. Haplotype structure and genotype-phenotype correlations of the sulfonyleurea receptor and the islet ATP-sensitive potassium channel gene region. *Diabetes* 2004;53:1360–1368
36. Gloy AL, Hashim Y, Ashcroft SJ, Ashfield R, Wiltshire S; UK Prospective Diabetes Study (UKPDS 53). Association studies of variants in promoter and coding regions of beta-cell ATP-sensitive K-channel genes *SUR1* and *Kir6.2* with Type 2 diabetes mellitus (UKPDS 53). *Diabet Med* 2001;18:206–212
37. Fatehi M, Raja M, Carter C, Soliman D, Holt A, Light PE. The ATP-sensitive K<sup>+</sup> channel *ABCC8* S1369A type 2 diabetes risk variant increases MgATPase activity. *Diabetes* 2012;61:241–249
38. Mianné J, Codner GF, Caulder A, et al. Analysing the outcome of CRISPR-aided genome editing in embryos: screening, genotyping and quality control. *Methods* 2017;121–122:68–76
39. Solomou A, Philippe E, Chabosseau P, et al. Over-expression of *Slc30a8/ZnT8* selectively in the mouse  $\alpha$  cell impairs glucagon release and responses to hypoglycemia. *Nutr Metab (Lond)* 2016;13:46
40. Ravier MA, Rutter GA. Isolation and culture of mouse pancreatic islets for ex vivo imaging studies with trappable or recombinant fluorescent probes. *Methods Mol Biol* 2010;633:171–184
41. Dholakia U, Bandyopadhyay S, Hod EA, Prestia KA. Determination of RBC survival in C57BL/6 and C57BL/6-Tg(UBC-GFP) mice. *Comp Med* 2015;65:196–201
42. Girard CA, Wunderlich FT, Shimomura K, et al. Expression of an activating mutation in the gene encoding the KATP channel subunit Kir6.2 in mouse pancreatic beta cells recapitulates neonatal diabetes. *J Clin Invest* 2009;119:80–90
43. Yi Y, Dongmei L, Phares DA, Weiss EP, Brandauer J, Hagberg JM. Association between *KCNJ11* E23K genotype and cardiovascular and glucose metabolism phenotypes in older men and women. *Exp Physiol* 2008;93:95–103
44. Shaat N, Ekelund M, Lernmark A, et al. Association of the E23K polymorphism in the *KCNJ11* gene with gestational diabetes mellitus. *Diabetologia* 2005;48:2544–2551
45. Weir GC, Bonner-Weir S. Islet  $\beta$  cell mass in diabetes and how it relates to function, birth, and death. *Ann N Y Acad Sci* 2013;1281:92–105
46. Haythorne E, Rohm M, van de Bunt M, et al. Diabetes causes marked inhibition of mitochondrial metabolism in pancreatic  $\beta$ -cells. *Nat Commun* 2019;10:2474
47. Koster JC, Marshall BA, Ensor N, Corbett JA, Nichols CG. Targeted over-activity of beta cell K(ATP) channels induces profound neonatal diabetes. *Cell* 2000;100:645–654
48. Wajchenberg BL. beta-Cell failure in diabetes and preservation by clinical treatment. *Endocr Rev* 2007;28:187–218
49. Shimajiri Y, Yamana A, Morita S, Furuta H, Furuta M, Sanke T. Kir6.2 E23K polymorphism is related to secondary failure of sulfonyleureas in non-obese patients with type 2 diabetes. *J Diabetes Investig* 2013;4:445–449
50. Rustenbeck I. Desensitization of insulin secretion. *Biochem Pharmacol* 2002;63:1921–1935